



A multiple charging correction algorithm for broad supersaturation scanning cloud condensation nuclei (BS2-CCN) system

Najin Kim^{1,2}, Hang Su¹, Nan Ma³, Ulrich Pöschl¹, Yafang Cheng²

¹Multiphase Chemistry Department, Max Planck Institute for Chemistry, Mainz, 55128, Germany

5 ²Minerva Research Group, Max Planck Institute for Chemistry, Mainz, 55128, Germany

³Center for Air Pollution and Climate Change Research (APCC), Institute for Environmental and Climate Research (ECI), Jinan University, Guangzhou, 511443, China

Correspondence to: Yafang Cheng (yafang.cheng@mpic.de)

Abstract. High time resolution (~ 1 s) of aerosol hygroscopicity and CCN activity can be obtained with a Broad Supersaturation Scanning Cloud Condensation Nuclei (BS2-CCN) system. Based on a commercial DMT-CCNC, the newly designed diffusive inlet in the BS2-CCN realizes a broad supersaturation distribution in a chamber with a stable low sheath to aerosol flow ratio (SARs). In this way, a monotonic relation between activation fraction of aerosols (F_{act}) and critical activation supersaturation ($S_{aerosol}$) can be obtained. The accuracy of the size-resolved aerosol hygroscopicity, κ , measured by the BS2-CCN system can be, however, hampered by multiply charged particles, i.e., resulting in the overestimation of κ values. As the BS2-CCN system uses multiple and continuous supersaturations in the chamber and the size-resolved F_{act} value is directly used to derive κ values, the multiple charging correction algorithm of the traditional CCNC where single supersaturation is applied does not work for the BS2-CCN observation. Here, we propose a new multiple charging correction algorithm to retrieve the true F_{act} value. Starting from the largest size bin, a new F_{act} value at a specific particle diameter (D_p) is updated from a measured activation spectra after removing both aerosol and CCN number concentration of multiply charged particles using a Kernel function with a given particle number size distribution. We compare the corrected activation spectra with laboratory aerosols for a calibration experiment and ambient aerosols during the 2021 Yellow-Sea Air Quality Studies (YES-AQ) campaign. The difference between corrected and measured κ values can be as large as 0.08 within the measured κ values between 0.11 and 0.37 among the selected samples, highlighting that multiple charge effect should be considered for the ambient aerosol measurement. Furthermore, we examine how particle number size distribution is linked to the deviation of activation spectra and κ values.

1 Introduction

Cloud condensation nuclei (CCN), the subset of atmospheric aerosol particles that can activate at certain supersaturation to form cloud droplets, are the key element in global climate change as they modulate the microphysical properties of the clouds (e.g., number concentration, mass and effective radius). Despite their scientific importance, there are still large uncertainties in assessing the aerosol-cloud interaction and quantification of their effect on climate due to the complexity of atmospheric



composition and processes. To reduce these uncertainties, knowledge of the spatio-temporal distribution of CCN and their activation characteristics is essential. As part of these efforts, numerous field campaigns have been carried out in the various regions over the past years (Andrae and Rosenfeld 2008; Chang et al., 2009; Che et al., 2016; Ervens et al., 2009; Gunthe et al., 2009; Hämeri et al., 2001; Hudson 1993; Jurányi et al., 2011; Kim et al., 2014; Moore et al., 2012; Ovadnevaite et al., 2011; Pöhlker et al., 2016; Rose et al., 2010; Schmale et al. 2018; Su et al., 2010; Thalman et al., 2017; Xu et al., 2021 and reference therein).

The activation of CCN at a given level of supersaturation can be primarily determined by particle size, followed by chemical composition and mixing state (Dusek et al., 2006; Ervens et al., 2009; Ren et al., 2018; Padró et al., 2012). Therefore, the size-resolved CCN measurement can separate the size effect to investigate the chemical composition effect on CCN activation efficiency under the simple assumption. This can help improve the understanding of CCN activation characteristics. Also, the critical diameter at a given supersaturation can be determined. For the size-resolved CCN measurement, a differential mobility analyzer (DMA) is commonly used to select the particle size before particles enter into the CCN Counter (CCNC). As particles passed through the DMA are not all singly charged under the given electrical mobility, numerous approaches have been proposed to correct multiply charged particles. Multiply charged particles with a larger size penetrate the DMA resulting in a higher CCN activation ratio than the actual value. Higher CCN activation ratio cause error when deriving the critical diameter and, thereby, κ value, a single hygroscopicity parameter (Petters and Kreidenweis 2007). Notably, the multiple charge effect is evident for ambient aerosols that show a large geometric diameter. Frank et al. (2006) proposed a correction method by removing the multiply charged particle fraction in number size distribution scaled by an activation efficiency of an average of five spectra. Petters et al. (2007) used an activation model of CCNC response of transferred polydisperse charged-equilibrated particles that pass through an ideal DMA. The activation efficiency of the particle distribution with the best estimate of critical diameter (D_c) is determined by minimizing the χ^2 statistic by varying the assumed D_c . Rose et al. (2008) simply assumed a constant fraction by doubly charged particle from the lower level of the plateau in the CCN efficiency spectra. Moore et al. (2010) used the algorithm for scanning mobility CCN analysis (SMCA). The activation fraction of set diameter, $R_a(D_p)$, is determined by removing total particle (i.e., condensation nuclei, CN) and CCN with +2 and +3 charges iteratively until convergence of $R_a(D_p)$. Ultimately, these methods are to find the true critical diameter or supersaturation that we want to obtain to derive the κ value.

The broad supersaturation scanning (BS2) CCN approach proposed by Su et al. (2016) modified the inlet and flow system of commercial CCNC to obtain aerosol hygroscopicity and CCN activity with a high time resolution. With a new monotonic relation between the activation fraction (F_{act}) and the activation supersaturation ($S_{aerosol}$), the κ value can be directly determined when the size-resolved CCN activation of set diameter is measured. Kim et al. (2021) implemented a BS2-CCN system and proposed a calibration method. With the CCN activation model, a response of CCNC with and without considering doubly charged particles was compared and suggested a method for calibration experiment to minimize the multiple charge effect. Although the calibration experiment can control particle size distribution to minimize this effect, multiple charging correction method is necessary when it is applied to the ambient aerosol measurement because particle size distribution cannot



65 be controlled and F_{act} directly affects the κ value in the BS2-CCN system. In other words, a high F_{act} value caused by multiply
charged particles of ambient aerosols results in an overestimation of κ value. However, several algorithms mentioned above
to correct the multiple charged particles cannot be directly applied to the BS2-CCN system. The reasons are as follows: 1)
BS2-CCN system uses multiple and continuous supersaturations in the chamber, not a single supersaturation used in
commercial DMT-CCNC. 2) The size-resolved F_{act} value is directly used to derive κ value, whereas original methods focus
70 on a critical diameter or supersaturation. 3) The CCN activation model proposed by Kim et al. (2021) is only applicable to a
known calibration aerosol. The model considers the multiple charge effect on total particle and CCN separately, which the
equation contains the transfer function for a cylindrical DMA column and the charge distribution of particles carrying
elementary charges. Particularly, for CCN, the function for a fraction of particles that activate as cloud droplets is added into
the equation and the information of $S_{aerosol}$ at a specific diameter is necessary. In other words, this model cannot be applied
75 to ambient aerosols with an unknown κ value. Therefore, we propose a multiple charging correction algorithm for the BS2-
CCN system in this paper. With a relevant theory for the electric mobility classifier, we summarize the procedure and show
examples of ambient aerosol measurement applying the algorithm.

2 Method

2.1 Basic theory: multi-charge effect

80 A particle with a narrow range of electrical mobility (Z_p) can pass through the DMA. The Z_p is defined as follows:

$$Z_p = \frac{veC(D_p)}{3\pi\mu D_p}, \quad (1)$$

Where e is the elementary charge, v is the number of elementary charges on the particle, $C(D_p)$ is the Cunningham slip
correction, μ is the dynamic viscosity of air. The mobility bandwidth, ΔZ_p , is:

$$\Delta Z_p = \frac{Q_a}{Q_{sh}} Z_p^*, \quad (2)$$

85 Where Q_{sh} and Q_a are the volumetric sheath flow and aerosol flow, respectively.

The particle charge distribution at each size can be calculated by a theoretical model that has been proposed by Wiedensohler
et al. (1986). We can calculate the probability that a particle will pass through a DMA classifier using the Kernel function,
 $G_v(D_p^*, x)$, as follows:

$$G_v(D_p^*, x) = \sum_{v=1}^{\infty} F(x, v) \Omega(x, v, D_p^*), \quad (3)$$

90 Where D_p^* is a set diameter in the DMA, x is the scale parameter, and $F(x, v)$ is the charge distribution of the particles with v
elementary charges, $\Omega(x, v, D_p^*)$ is the probability of particles of D_p^* that pass through the DMA. It considers the electrical
mobility and the mobility bandwidth for a given diameter and flow ratio.



2.2 Multiple charging correction algorithm for BS2-CCN

Based on the theory, we present the procedure of a multiple charge correction algorithm for the BS2-CCN system. As the κ value is calculated directly from F_{act} , the algorithm aims at deriving true F_{act} we want to obtain from observed F_{act} . The experimental setup for the size-resolved CCN measurement is described in Kim et al. (2021). Selected dry particles by DMA split into two ways, CPC for particle number concentration and a modified CCNC for CCN number concentration. Scanning the size of particles with an F_{act} of 0 to 1 is performed, and the algorithm applies starting from larger particle to small particle.

1. The CN and CCN number size distribution, $C_{CN}(D_p)$ and $C_{CCN}(D_p)$, are obtained by the inversion of CN time series and CCN time series (here using the own private software).
2. The size-dependent activation fraction, $F_{act}(D_p) = C_{CCN}(D_p)/C_{CN}(D_p)$, is obtained from CN and CCN time series. For each particle diameter, $F_{act}(D_p)$ is calculated by averaging 25s data excluding the stabilization time of 15s. The original time resolution of the CN and CCN time series is 1s.
3. The $F_{act}(D_p)$ values between set particle sizes can be obtained through interpolation. The $F_{act}(D_p)$ of particle size larger than the largest D_p is assumed to be 1.0. It is noted that $F_{act}(D_p)$ of largest particle size is to be 1.0.
4. Starting from the largest aerosol size bin, particle number concentration of single charge that can pass through DMA (set D_p^*) is calculated by Kernel function with a given particle number size distribution, $n(x)$ after removing the number concentration of particles with +2 and +3 (or more) charges using Eq. (4).

$$N_v(D_p^*) = \int_0^\infty G_v(D_p^*, x)n(x)dx, \quad (4)$$

5. As CCN number concentration can be calculated with the product of F_{act} and N_v , we can calculate true F_{act} value, F_{act}^* , by subtracting the CCN number concentration by multiply charged particles from the measured CCN number concentration. To be specific, CCN number concentration of multiply charged particles can be calculated with information of particle diameter of +2 and +3 (or more) charges and corresponding F_{act} from F_{act} curve (Eq. 5). It is noted that $h(x, v, D_p^*)$ is a mathematical form of an activated fraction, F_{act} , function for D_p^* with v elementary charges.

$$N_{CCN}(D_p^*) = \int_{v=1}^\infty \int_0^\infty G_v(D_p^*, x)h(x, v, D_p^*)n(x) dx dv, \quad (5)$$

6. The calculated $F_{act}^*(D_p^*)$ that we want to obtain in step (5) is updated to the existing F_{act} function, $h(x, v, D_p^*)$.
7. Repeat step (3)- (6) from the largest to the smallest diameter.

Through the single process, Step (3) – (6), we obtain the $F_{act}^*(D_p^*)$ value, and the calculated $F_{act}^*(D_p^*)$ is reflected into the $D_p - F_{act}$ curve which is used in the calculation process of the following particle size.

Figure 1 shows the calculated Kernel function for the DMA (TSI 3080) set the size of 70 nm with different charges ($v = 1, 2, 3$). It is noted that particles carrying more than three charges within the particle size range in ambient air are not considered in this study. The sample/sheath flow ratio of 1.5/10 is applied for calculation, the same setting for calibration experiment and



125 ambient aerosol measurement, mainly discussed in Section 4. Kernel function can be different with the sample/sheath flow
ratio. Particle number concentration carrying a specific charge can be determined by Kernel function and particle number size
distribution (Eq. 4). Figure 2 shows particle number fraction at each charge under an assumed particle distribution data obtained
from ambient aerosol measurement. According to Fig.2, most particles are composed of particles with a single or double
charge, but the particle number fraction by triple charge between 60 nm and 90 nm, where the particle number concentration
is high, was also slightly seen. The number concentrations by singly charged particles were dominant, but there was a size
130 range where a number fraction by doubly charged particles was more than 0.1. It means that in a region where larger particles
are dominant, the effect of a doubly charged particle would be more prominent, and thereby it is necessary to apply the multiple
charging correction algorithm.

3 Application

135 The multiple charge correction algorithm is applied to the calibration experiment and ambient aerosol measurements. Before
applying the algorithm, a log-normal fitting procedure for aerosol number concentration is conducted to calculate the number
concentration of particles by double and triple charges as described in Eq. (4) and (5). It is well known that the size distribution
of atmospheric aerosols can be expressed by a log-normal distribution, and other fitting functions can be used if the number
size distribution cannot be described by the log-normal distribution.

140 3.2 Calibration experiment

Calibration experiments for the BS2-CCN system are performed with ammonium sulfate, well-known calibration aerosols for
CCNC under the $dT=6\text{ K}$ and 8 K conditions. An instrumental setting of the calibration experiment is the same as the existing
BS2-CCN system except that an atomizer for generating a calibration aerosol is added to the front of the DMA. Details are
described in Kim et al. (2021). Figure 3 shows the aerosol and CCN number size distribution, activation fraction (F_{act}) curve
145 and BS2-CCN calibration curve under the two dT conditions. According to Fig.3a, CCN number size distribution shows a
small plateau in the front by multiply charged particles leading to the small plateau of F_{act} (Fig. 3b). When applying the
algorithm, this small plateau disappears, and the other F_{act} value slightly decrease. The results show that the algorithm corrects
the increased F_{act} values due to multiple charge particles. The elevated F_{act} values induced by multiply charged particles in
Fig.3 are not that high, less than 0.1, due to the small geometric mean diameter (D_g) and standard deviation (σ_g) of a generated
150 particle number size distribution. It is the way to minimize the effect of multiply charged particles on the calibration curve
(Kim et al. 2021). Figure 3a and Table 1 show the calibration curve, coefficients of the fitted calibration curve, and goodness
of fit before and after the correction. There is no significant difference in each coefficient and the shape of the calibration
curve. The reasons for this are as follows: 1) For the fitting procedure, values lower than 0.05 of F_{act} value where small plateau
by multiply charged particle exists are excluded. 2) Calibration experiment presented in this section follows the



155 recommendation suggested by Kim et al. (2021) to generate particle size distribution with small D_g and σ_g and thereby, the
effect of multiply charged particles is not that obvious. 3) $F_{act} - S_{aerosol}$ relation is determined based on $\kappa - Köhler$ theory
(Petters and Kridenweis, 2007). In other words, the value of $S_{aerosol}$ changes based on the theory according to the reduced
 F_{act} . It can be inferred from these results that the suggested algorithm corrects the F_{act} induced by doubly and triply charged
160 charged particles can be minimized, and almost the same calibration curve can be obtained without correction if the
experimental control is performed well.

3.3 Ambient aerosol

Unlike calibration aerosols, particle number size distribution of ambient aerosols cannot be controlled and D_g is generally
larger than lab-generating aerosols. Also, particle number size distribution is highly variable depending on time and region. It
165 means that F_{act} can be easily affected by multiply charged particles, so the correction algorithm is essential. Here, we adopted
two cases from polluted marine aerosol measurement that was held in the Yellow Sea during springtime, 2021. Details of field
campaign measurement will be covered in another paper. As in Section 4.1, the measured aerosol number concentration data
were fitted to the log-normal distribution for calculation. Figure 4 shows the measured aerosol and CCN number size
distribution and the activation curve before and after the correction of Case I. D_g and σ_g are 70.6 nm and 1.58, respectively.
170 When applying the algorithm, the F_{act} decreases from 0.01 to 0.07, and the F_{act} value decreases the most in the 70 nm where
the particle number concentration is the highest. Figure 5 is the same as Fig. 4 with Case II, larger D_g and higher σ_g than Case
I ($D_g = 129.0$ nm and $\sigma_g = 1.65$). As the peak diameter becomes larger, the effect of multiply charged particles increases. The
 F_{act} decreases by up to 0.2. Although N_{CCN} by doubly charged particle shows the maximum near the peak of N_{CN} , the decrease
in the value of F_{act} was dominant in the range where F_{act} is 0.1 to 0.8, and the corresponding particle size was smaller than
175 the peak diameter. It is because F_{act} is calculated not only by N_{CCN} but also by N_{CN} after subtracting multiply charged particles.
Also, when calculating N_{CCN} , the original F_{act} from the measurement is considered. Figure 6 shows the change of κ value
according to the change of F_{act} . In Case II, since the decrease in F_{act} is more prominent than in Case I, the difference in κ
value after the correction is also more significant. For Case II, the change in the κ value is about 0.04 to 0.08, whereas for Case
I, the change in κ is about 0.01. We can conclude from these results that the effect of multiply charged particle is different
180 with particle number size distribution. And, the difference in κ of 0.08 can lead to a relative deviation of CCN number
concentration of up to about 20% when assuming the particle size distribution of Case II and supersaturation ranging from
0.05 to 1.0%. It means that the correction algorithm should be applied if the peak size of ambient aerosols is large and has a
broad particle number size distribution.



4 Discussion and conclusion

185 As discussed above, F_{act} by multiply charged particle can affect the activation spectra and thereby the κ derivation. The extents of F_{act} and κ deviation between original and corrected activation spectra (i.e., $D_p - F_{act}$) for Case I and Case II were different due to the different particle number size distribution. Therefore, we further examined how particle number size distribution is linked to the deviation of activation spectra and κ values. Based on the observed activation spectra, referred to as ‘original’, we applied the correction algorithm by changing D_g of particle size distribution. The value obtained by applying the algorithm

190 refers to as ‘corrected’. The relative deviation is defined as the difference between the original and corrected value. Figure 7 is a contour plot of the relative deviation of F_{act} and κ as function of D_g for the log-normally fitted particle size distribution for Case I and Case II. The red dashed line indicates the original D_g of each Case as described in Section 3.3. For Case I (Fig.7a), the maximum value appears near the original D_g , 70nm, and gradually decreases. As D_g increases, the relative deviation of F_{act} increases, and the interval between the contour also gradually narrows. It is noted that deviation values

195 between 60 and 120 nm in D_p which correspond to F_{act} value between 0.1 and 0.9 are meaningful. The deviation of κ value in Fig. 7b also showed a similar tendency to that of F_{act} value. For Case II (Fig. 7c), the maximum relative deviation value appears near the 60 nm. The relative deviation value of F_{act} is higher and the interval is narrower than Case I. It can be explained by the original particle number size distribution and activation spectra in Fig.4 and 5. Case II shows a much broader and larger particle size distribution, which means the effect of multiply charged particle is larger in Case II. Also, F_{act} shows

200 a higher value at the same particle size in Case II than Case I implying different chemical composition due to different air masses. For Case II, deviation values between 50 and 100 nm in D_p which correspond to F_{act} value between 0.1 and 0.9 are meaningful. Like Case I, Case II also shows that the deviation of F_{act} increases as D_g increases, and the deviation of κ also tends to be similar (Fig.7c and 7d). It means that change in particle size distribution affect the deviation of F_{act} and thereby κ value regardless of the original activation spectra.

205 In summary, we propose a multiple charging correction algorithm for the BS2-CCN system with continuous and multiple supersaturations in the chamber. Unlike existing algorithms, the correction algorithm in this study aims at deriving the true value of F_{act} at each particle size as F_{act} value is used to derive κ directly. Starting from larger particles, number concentrations of particles both N_{CN} and N_{CCN} with multiple charges (here, we consider only +2 and +3 charges) are removed, and new F_{act} is updated to the original activation spectra. The same procedure is repeated to the smaller particle after updating new F_{act}

210 value. When applying the algorithm, the F_{act} value was corrected, especially in the range between 0.1 and 0.9 of F_{act} and the plateau in activation spectra by multiply charged particles was successfully eliminated. The extent of correction depends on the particle size distribution. To be specific, there is no large discrepancy of activation spectra and calibration curve (i.e., $F_{act} - S_{aerosol}$ relation) if the particle size distribution of generated calibration aerosols is well controlled with smaller D_g . For ambient aerosols, larger deviations of F_{act} and κ were shown with larger D_g . The difference between corrected and original

215 κ values of 0.08 from samples could lead to about 20% of the relative deviation of CCN number concentration within the



supersaturation range between 0.05 and 1.0%, which cannot be ignored. It can be concluded that the multiple charge correction algorithm should be applied to the ambient aerosols with a variety of particle number size distributions to reduce the error when calculating the κ value in the BS2-CCN system.



220 **Code and data availability**

Algorithm code and data can be available upon request from the corresponding author (yafang.cheng@mpic.de).

Author contributions

NK designed and implemented the data correction algorithm for BS2-CCN system. YC supervised and led the paper preparation. HS and NM contributed to the discussion with their expertise in BS2-CCN system and measurement data
225 processing. NK wrote the paper. All coauthors discussed and results and commented on the paper.

Competing interests

At least one of the (co-)authors is a member of the editorial board of *Atmospheric Measurement Techniques*.

Acknowledgments

This work was supported by the Max Planck Society (MPG). Y.C. and N.K. thank the support from Minerva Program from
230 MPG.



References

- 235 Andreae, M. O. and Rosenfeld, D.: Aerosol-cloud-precipitation interactions. Part 1, The nature and sources of cloud-active aerosols, *Earth Sci. Rev.*, 89, 13–41, 2008.
- Chang, R. Y.-W., Slowik, J. G., Shantz, N. C., Vlasenko, A., Liggio, J., Sjostedt, S. J., Leaitch, W. R., and Abbatt, J. P. D.: The hygroscopicity parameter (κ) of ambient organic aerosol at a field site subject to biogenic and anthropogenic influences: Relationship to degree of aerosol oxidation, *Atmos. Chem. Phys. Discuss.*, 9, 25323–25360, 2009
- 240 Che, H. C., Zhang, X. Y., Wang, Y. Q., Zhang, L., Shen, X. J., Zhang, Y. M., Ma, Q. L., Sun, J. Y., Zhang, Y. W., and Wang, T. T.: Characterization and parameterization of aerosol cloud condensation nuclei activation under different pollution conditions, *Scient. Rep.*, 6, 24497, <https://doi.org/10.1038/srep24497>, 2016.
- Dusek, U., Frank, G. P., Hildebrandt, L., Curtius, J., Schneider, J., Walter, S., Chand, D., Drewnick, F., Hings, S., Jung, D., Borrmann, S., and Andreae, M. O.: Size matters more than chemistry for cloud nucleating ability of aerosol particles, *Science*, 312, 1375–1378, 2006.
- 245 Ervens, B., Cubison, M. J., Andrews, E., Feingold, G., Ogren, J. A., Jimenez, J. L., Quinn, P. K., Bates, T. S., Wang, J., Zhang, Q., Coe, H., Flynn, M., and Allan, J. D.: CCN predictions using simplified assumptions of organic aerosol composition and mixing state: a synthesis from six different locations, *Atmos. Chem. Phys. Discuss.*, 9, 21237–21256, 2009, <http://www.atmos-chem-phys-discuss.net/9/21237/2009/>.
- Frank, G. P., Dusek, U., and Andreae, M. O.: Technical Note: A Method for Comparing Size-Resolved CCN in the
250 Atmosphere, *Atmos. Chem. Phys. Discuss.* 6:4879–4895, 2006.
- Gunthe, S. S., King, S. M., Rose, D., Chen, Q., Roldin, P., Farmer, D. K., Jimenez, J. L., Artaxo, P., Andreae, M. O., Martin, S. T., and Poschl, U.: Cloud condensation nuclei in pristine tropical rainforest air of Amazonia: size-resolved measurements and modeling of atmospheric aerosol composition and CCN activity, *Atmos. Chem. Phys.*, 9, 7551–7575, 2009, <http://www.atmos-chem-phys.net/9/7551/2009/>.
- 255 Hämeri, K., Väkevä, M., Aalto, P. P., Kulmala, M., Swietlicki, E., Zhou, J., Seidl, W., Becker, E., and O'Dowd, C. D.: Hygroscopic and CCN properties of aerosol particles in boreal forests, *Tellus B*, 53, 359–379, 2001.
- Hudson, J. G.: Cloud condensation nuclei, *J. Appl. Meteorol.*, 32, 596–607, 1993.
- Jurányi, Z., Gysel, M., Weingartner, E., Bukowiecki, N., Kammermann, L., and Baltensperger, U.: A 17 month climatology of the cloud condensation nuclei number concentration at the high alpine site Jungfraujoch, *J. Geophys. Res.-Atmos.*, 116, D10204, <https://doi.org/10.1029/2010JD015199>, 2011.
- 260 Kim, N., Cheng, Y., Ma, N., Pöhlker, M. L., Klimach, T., Mentel, T. F., Krüger, O. O., Pöschl, U., and Su, H.: Calibration and evaluation of a broad supersaturation scanning (BS2) cloud condensation nuclei counter for rapid measurement of particle hygroscopicity and cloud condensation nuclei (CCN) activity, *Atmos. Meas. Tech.*, 14, 6991–7005, <https://doi.org/10.5194/amt-14-6991-2021>, 2021.



- 265 Kim, J. H., Yum, S. S., Shim, S., Kim, W. J., Park, M., Kim, J.-H., Kim, M.-H., and Yoon, S.-C.: On the submicron aerosol distributions and CCN number concentrations in and around the Korean Peninsula, *Atmos. Chem. Phys.*, 14, 8763–8779, <https://doi.org/10.5194/acp-14-8763-2014>, 2014.
- Moore, R. H., Cerully, K., Bahreini, R., Brock, C. A., Middlebrook, A. M., and Nenes, A.: Hygroscopicity and composition of California CCN during summer 2010, *J Geophys Res Atmospheres* 1984 2012, 117, n/a-n/a,
270 <https://doi.org/10.1029/2011jd017352>, 2012.
- Moore, R. H., Nenes, A. and Medina, J.: Scanning Mobility CCN Analysis – A Method for Fast Measurement of Size-Resolved CCN Distributions and Activation Kinetics, *Aerosol Sci. Tech.*, 44:10, 861-871, <https://doi.org/10.1080/02786826.2010.498715>, 2010.
- Ovadnevaite, J., Ceburnis, D., Martucci, G., Bialek, J., Monahan, C., Rinaldi, M., Facchini, M. C., Berresheim, H., Worsnop, D. R., and O’Dowd, C.: Primary marine organic aerosol: A dichotomy of low hygroscopicity and high CCN activity, *Geophys Res Lett*, 38, n/a-n/a, <https://doi.org/10.1029/2011gl048869>, 2011.
- Padró, L. T., Moore, R. H., Zhang, X., Rastogi, N., Weber, R. J., and Nenes, A.: Mixing state and compositional effects on CCN activity and droplet growth kinetics of size-resolved CCN in an urban environment, *Atmos. Chem. Phys.*, 12, 10239–10255, <https://doi.org/10.5194/acp-12-10239-2012>, 2012.
- 280 Petters, M. D. and Kreidenweis, S. M.: A single parameter representation of hygroscopic growth and cloud condensation nucleus activity, *Atmos. Chem. Phys.*, 7, 1961–1971, doi:10.5194/acp-7-1961-2007, 2007.
- Petters, M. D., Carrico, C. M., Kreidenweis, S. M., Prenni, A. J., DeMott, P. J., Collett Jr., J. L., and Moosmuller, H.: Cloud condensation nucleation activity of biomass burning aerosol, *J. Geophys. Res.*, 114, D22205, doi:10.1029/2009jd012353, 2009.
- 285 Pöhlker, M. L., Pöhlker, C., Ditas, F., Klimach, T., Hrabe de Angelis, I., Araújo, A., Brito, J., Carbone, S., Cheng, Y., Chi, X., Ditz, R., Gunthe, S. S., Kesselmeier, J., Könemann, T., Lavric, J. V., Martin, S. T., Mikhailov, E., Moran-Zuloaga, D., Rose, D., Saturno, J., Su, H., Thalman, R., Walter, D., Wang, J., Wolff, S., Barbosa, H. M. J., Artaxo, P., Andreae, M. O., and Pöschl, U.: Long-term observations of cloud condensation nuclei in the Amazon rain forest – Part 1: Aerosol size distribution, hygroscopicity, and new model parametrizations for CCN prediction, *Atmos. Chem. Phys.*, 16, 15709–15740, <https://doi.org/10.5194/acp-16-15709-2016>, 2016.
- 290 Ren, J., Zhang, F., Wang, Y., Collins, D., Fan, X., Jin, X., Xu, W., Sun, Y., Cribb, M., and Li, Z.: Using different assumptions of aerosol mixing state and chemical composition to predict CCN concentrations based on field measurements in urban Beijing, *Atmos. Chem. Phys.*, 18, 6907–6921, <https://doi.org/10.5194/acp-18-6907-2018>, 2018.
- Rose, D., Gunthe, S. S., Mikhailov, E., Frank, G. P., Dusek, U., Andreae, M. O., and Pöschl, U.: Calibration and measurement uncertainties of a continuous-flow cloud condensation nuclei counter (DMT-CCNC): CCN activation of ammonium sulfate and sodium chloride aerosol particles in theory and experiment, *Atmos. Chem. Phys.*, 8, 1153–1179, <https://doi.org/10.5194/acp-8-1153-2008>, 2008.



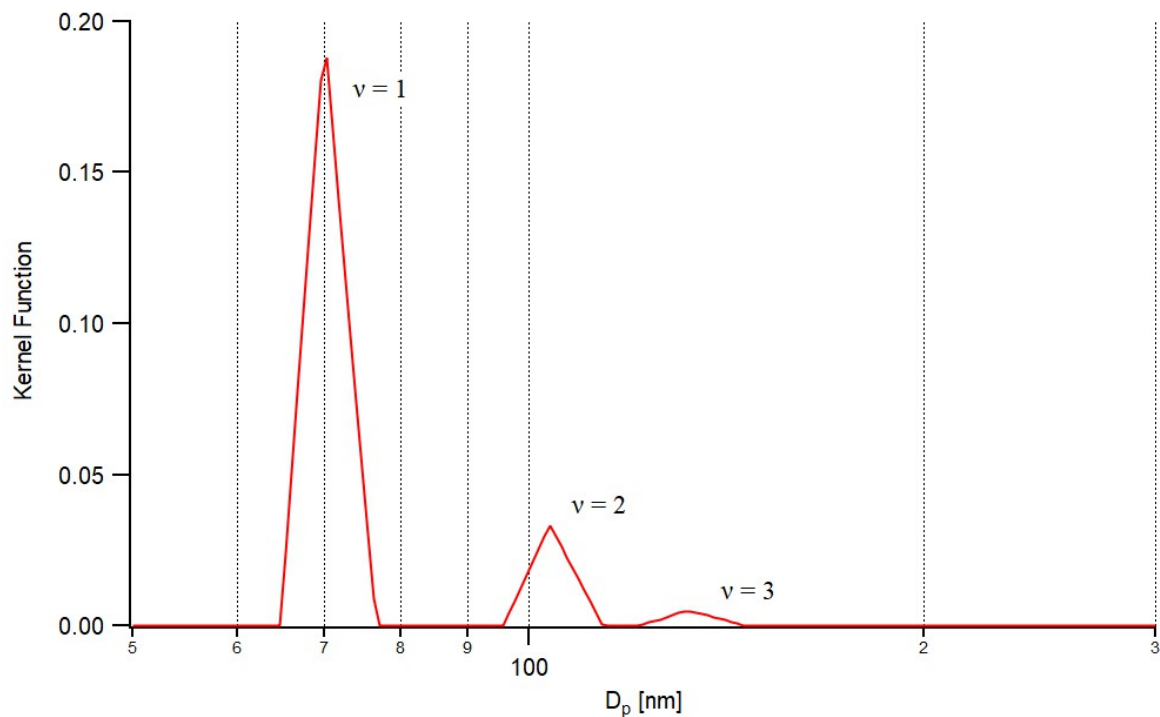
- Rose, D., Nowak, A., Achtert, P., Wiedensohler, A., Hu, M., Shao, M., Zhang, Y., Andreae, M. O., and Pöschl, U.: Cloud condensation nuclei in polluted air and biomass burning smoke near the mega-city Guangzhou, China – Part 1: Size-resolved measurements and implications for the modeling of aerosol particle hygroscopicity and CCN activity, *Atmos. Chem. Phys.*, 10, 3365–3383, <https://doi.org/10.5194/acp-10-3365-2010>, 2010.
- Schmale, J., Henning, S., Decesari, S., Henzing, B., Keskinen, H., Sellegri, K., Ovadnevaite, J., Pöhlker, M. L., Brito, J., Bougiatioti, A., Kristensson, A., Kalivitis, N., Stavroulas, I., Carbone, S., Jefferson, A., Park, M., Schlag, P., Iwamoto, Y., Aalto, P., Äijälä, M., Bukowiecki, N., Ehn, M., Frank, G., Fröhlich, R., Frumau, A., Herrmann, E., Herrmann, H., Holzinger, R., Kos, G., Kulmala, M., Mihalopoulos, N., Nenes, A., O'Dowd, C., Petäjä, T., Picard, D., Pöhlker, C., Pöschl, U., Poulain, L., Prévôt, A. S. H., Swietlicki, E., Andreae, M. O., Artaxo, P., Wiedensohler, A., Ogren, J., Matsuki, A., Yum, S. S., Stratmann, F., Baltensperger, U., and Gysel, M.: Long-term cloud condensation nuclei number concentration, particle number size distribution and chemical composition measurements at regionally representative observatories, *Atmos. Chem. Phys.*, 18, 2853–2881, <https://doi.org/10.5194/acp-18-2853-2018>, 2018.
- Su, H., Cheng, Y., Ma, N., Wang, Z., Wang, X., Pöhlker, M. L., Nillius, B., Wiedensohler, A., and Pöschl, U.: A broad supersaturation scanning (BS2) approach for rapid measurement of aerosol particle hygroscopicity and cloud condensation nuclei activity, *Atmos. Meas. Tech.*, 9, 5183–5192, <https://doi.org/10.5194/amt-9-5183-2016>, 2016.
- Su, H., Rose, D., Cheng, Y. F., Gunthe, S. S., Massling, A., Stock, M., Wiedensohler, A., Andreae, M. O., and Pöschl, U.: Hygroscopicity distribution concept for measurement data analysis and modeling of aerosol particle mixing state with regard to hygroscopic growth and CCN activation, *Atmos Chem Phys*, 10, 7489–7503, <https://doi.org/10.5194/acp-10-7489-2010>, 2010.
- Thalman, R., de Sá, S. S., Palm, B. B., Barbosa, H. M. J., Pöhlker, M. L., Alexander, M. L., Brito, J., Carbone, S., Castillo, P., Day, D. A., Kuang, C., Manzi, A., Ng, N. L., Sedlacek III, A. J., Souza, R., Springston, S., Watson, T., Pöhlker, C., Pöschl, U., Andreae, M. O., Artaxo, P., Jimenez, J. L., Martin, S. T., and Wang, J.: CCN activity and organic hygroscopicity of aerosols downwind of an urban region in central Amazonia: seasonal and diel variations and impact of anthropogenic emissions, *Atmos. Chem. Phys.*, 17, 11779–11801, <https://doi.org/10.5194/acp-17-11779-2017>, 2017.
- Xu, W., Fossom, K. N., Ovadnevaite, J., Lin, C., Huang, R.-J., O'Dowd, C., and Ceburnis, D.: The impact of aerosol size-dependent hygroscopicity and mixing state on the cloud condensation nuclei potential over the north-east Atlantic, *Atmos Chem Phys*, 21, 8655–8675, <https://doi.org/10.5194/acp-21-8655-2021>, 2021.



Table 1: Coefficients and goodness of fit for calibration curves for $dT = 8$ K condition before and after applying the multiple charge correction algorithm. Three different statistical values are used for goodness of fit: Error sum of squares (SSE), coefficient determination (R^2), and root mean square error (RMSE).

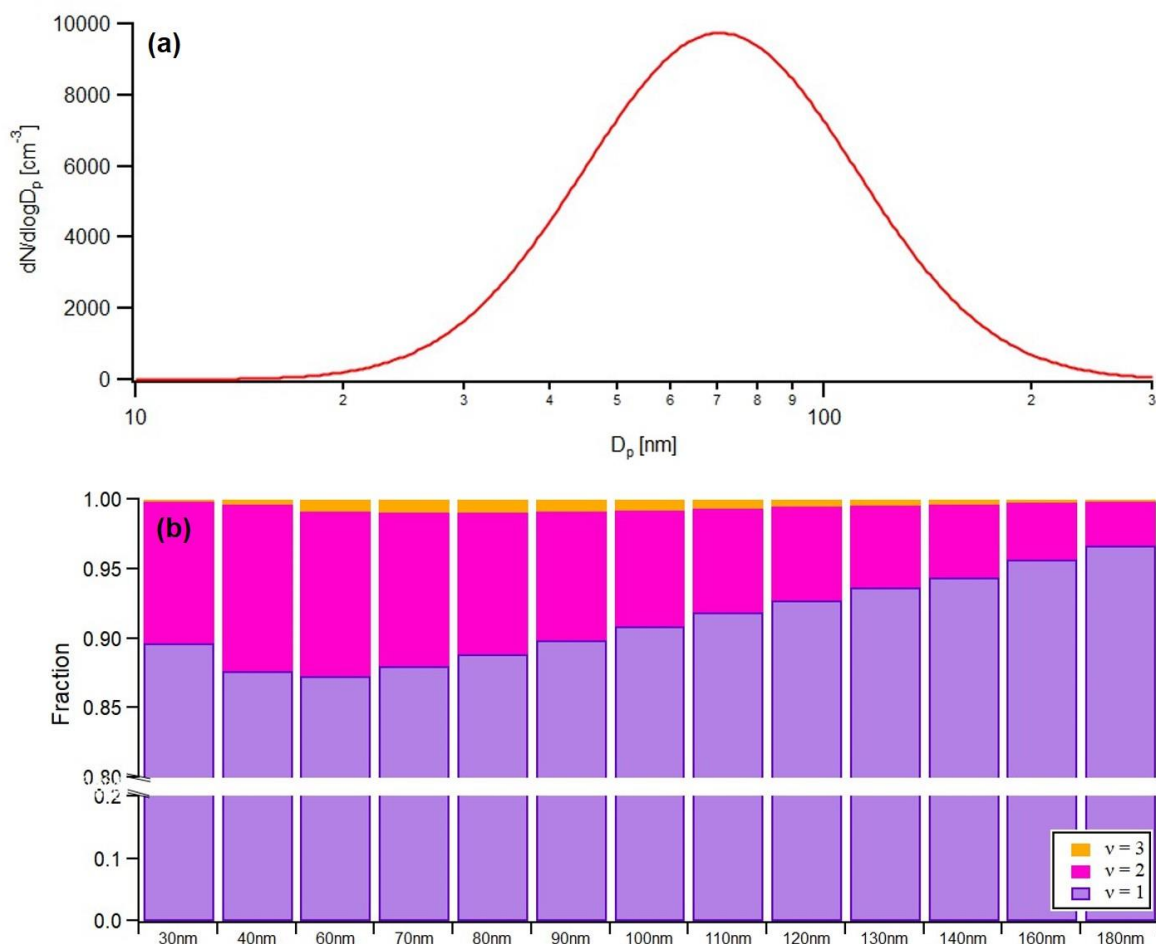
Equation	$F(x) = a \times \text{acos}(b \times x) - c$	
	Before the correction	After the correction
Coefficient (with 95% confidence bounds)	$a = 0.4056$ (0.3790, 0.4322) $b = 0.9534$ (0.9307, 0.9760) $c = 0.0464$ (0.0142, 0.0786)	$a = 0.3994$ (0.3710, 0.4277) $b = 0.9468$ (0.9201, 0.9736) $c = 0.0554$ (0.0198, 0.0910)
Goodness of fit	SSE = 0.000403 $R^2 = 0.9983$ RMSE = 0.005565	SSE = 0.000421 $R^2 = 0.9982$ RMSE = 0.005694

Coefficients and goodness of fit were calculated by the MATLAB curve fitting toolbox 3.5.8.



330

Figure 1: Kernel function for the DMA set size of 70 nm with different charges ($v = 1, 2, 3$). The sample/sheath flow rate is 1.5/10.



335 **Figure 2: (a) Lognormally fitted particle number size distribution ($D_g = 70.6 \text{ nm}$, $\sigma_g = 1.57$) and (b) particle number fraction at each charge to which the particle number size distribution is applied. Each color indicates charge number: Purple for singly charged particles ($v = 1$), pink for doubly charged particles ($v = 2$) and orange for triply charged particles ($v = 3$).**

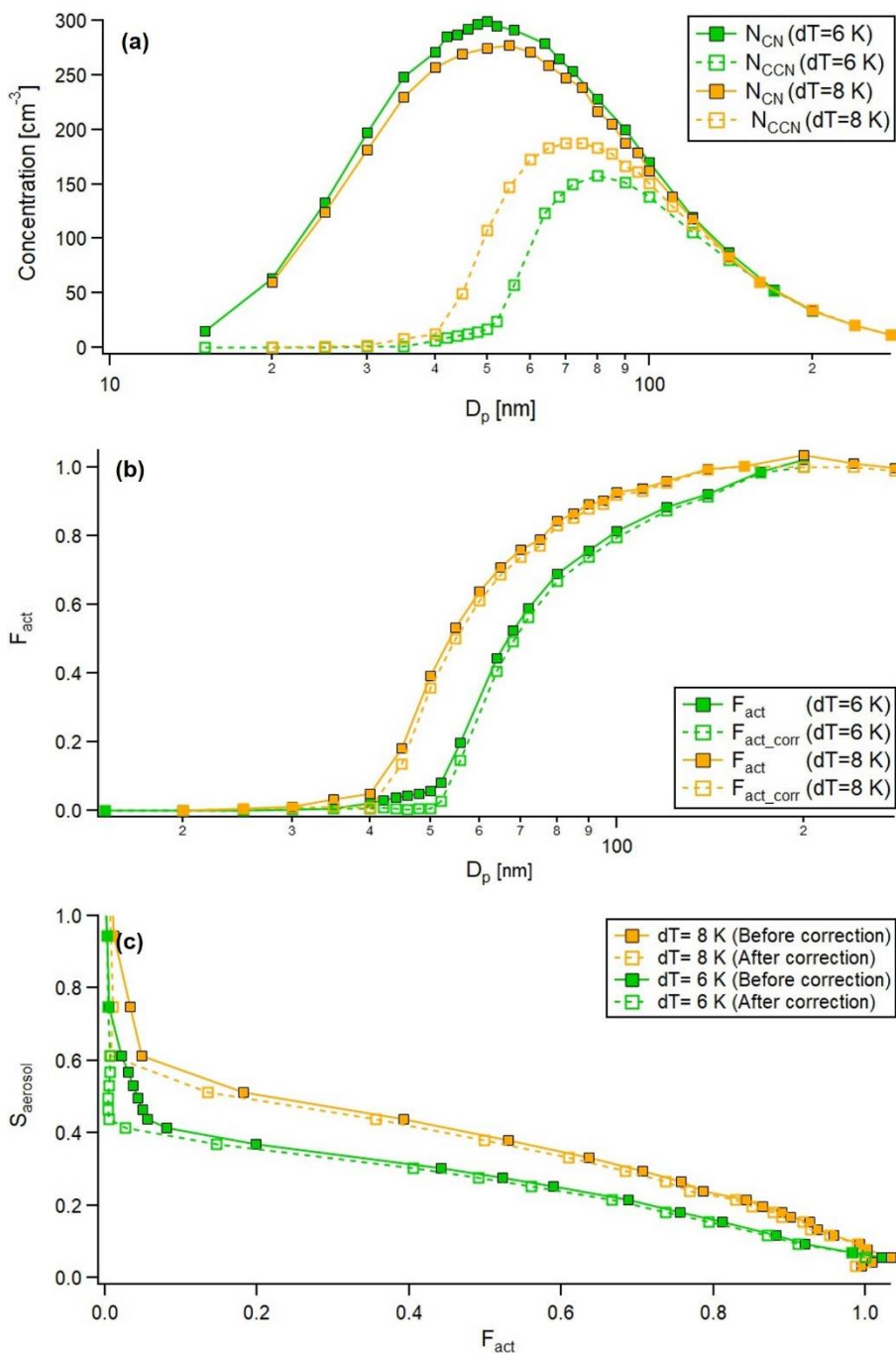


Figure 3: (a) Particle and CCN number size distribution (b) activation fraction (F_{act}) curve and (c) $F_{\text{act}} - S_{\text{aerosol}}$ calibration curve for $dT = 6$ K (green) and 8 K (orange). Squares indicate measurement points. Solid line and dashed line with squares indicate results before and after the correction, respectively.

340

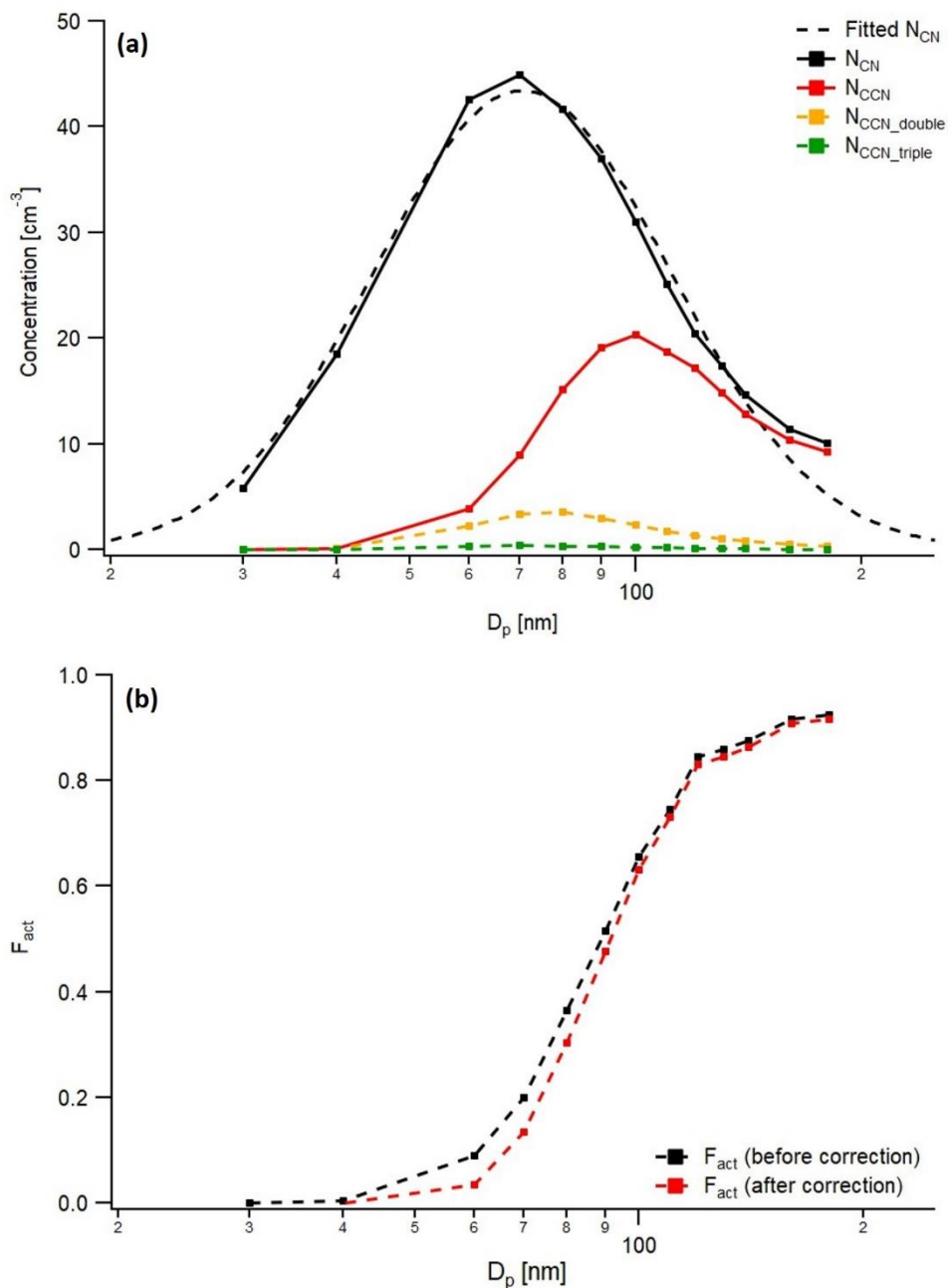


Figure 4: (a) Number size distribution of aerosol (black) and CCN (Red for total particle, Orange for doubly charged particle and Green for triply charged particle) and log-normally fitted particle number size distribution ($D_g = 70.6$ nm and $\sigma_g = 1.58$, black dashed line), and (b) activation curve before (black) and after correction (red) for Case I. Each dot indicates measurement point.

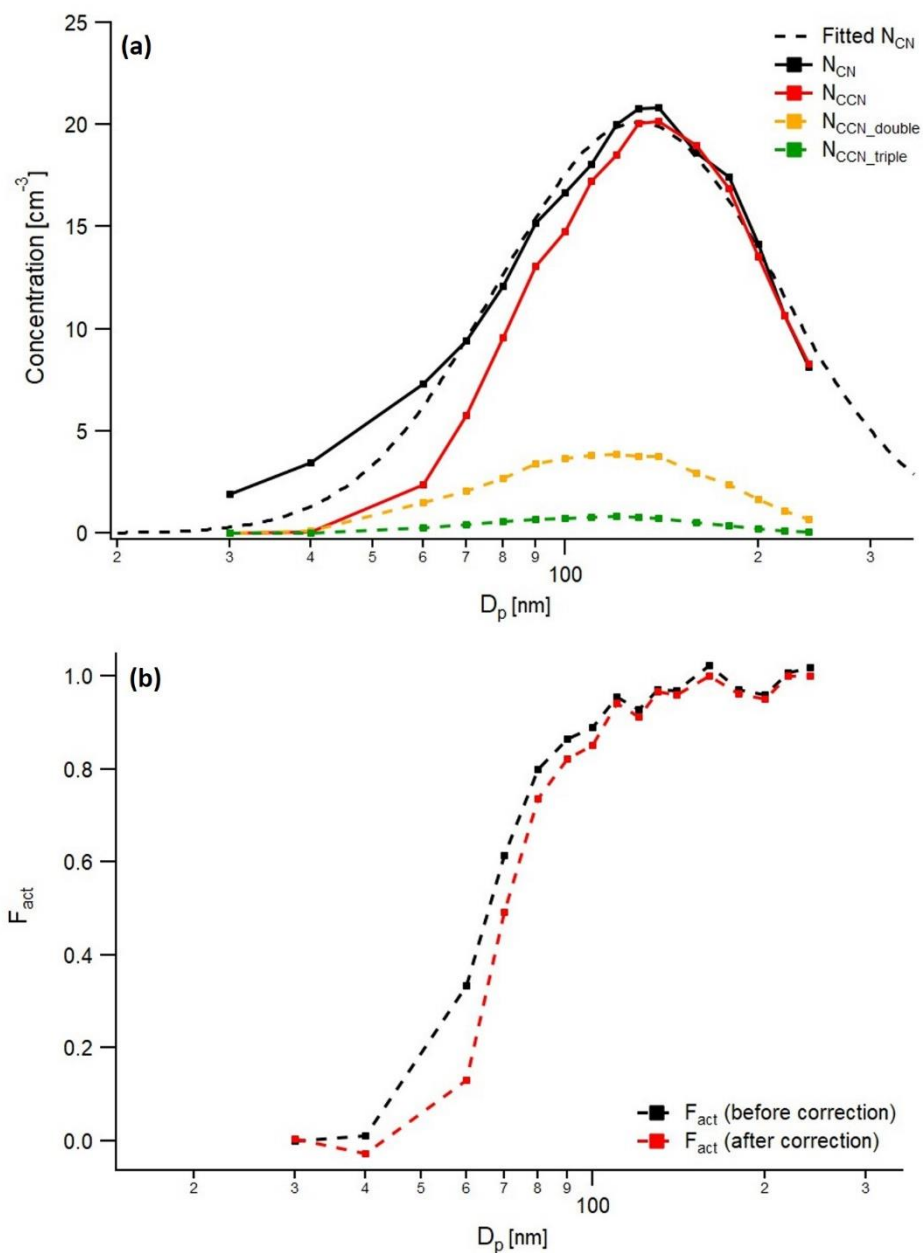


Figure 5: (a) Number size distribution of aerosol (black) and CCN (Red for total particle, Orange for doubly charged particle and Green for triply charged particle) and log-normally fitted particle number size distribution ($D_g = 129.0$ nm and $\sigma_g = 1.65$, black dashed line), and (b) activation curve before (black) and after correction (red) for Case II. Each dot indicates measurement point.

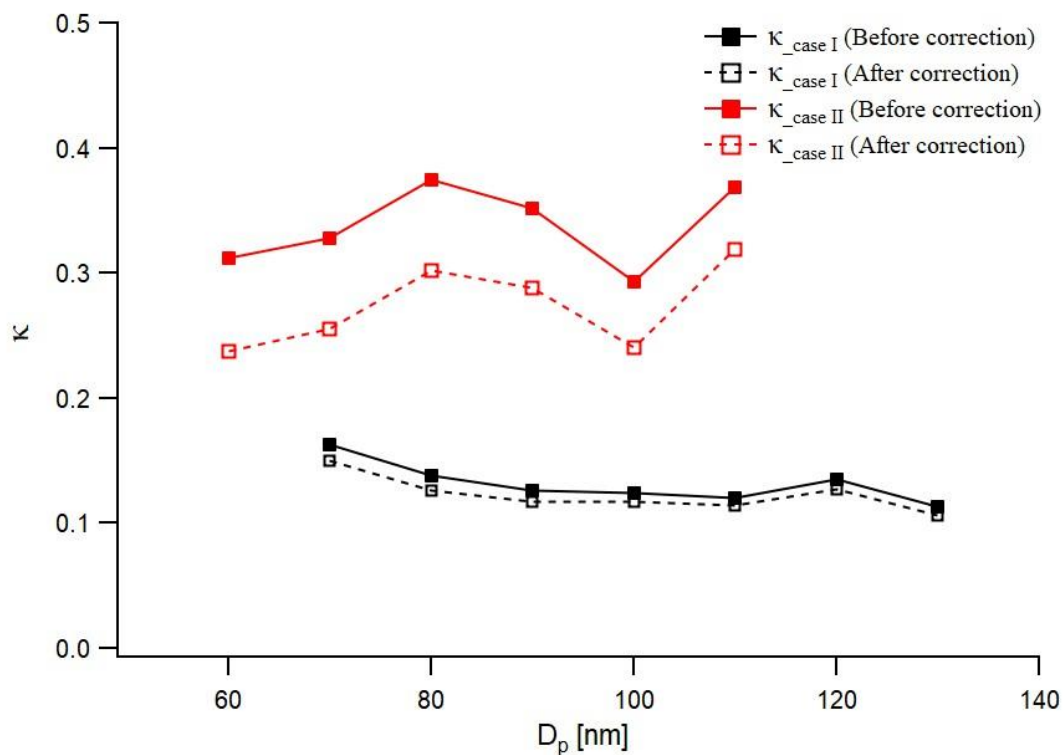
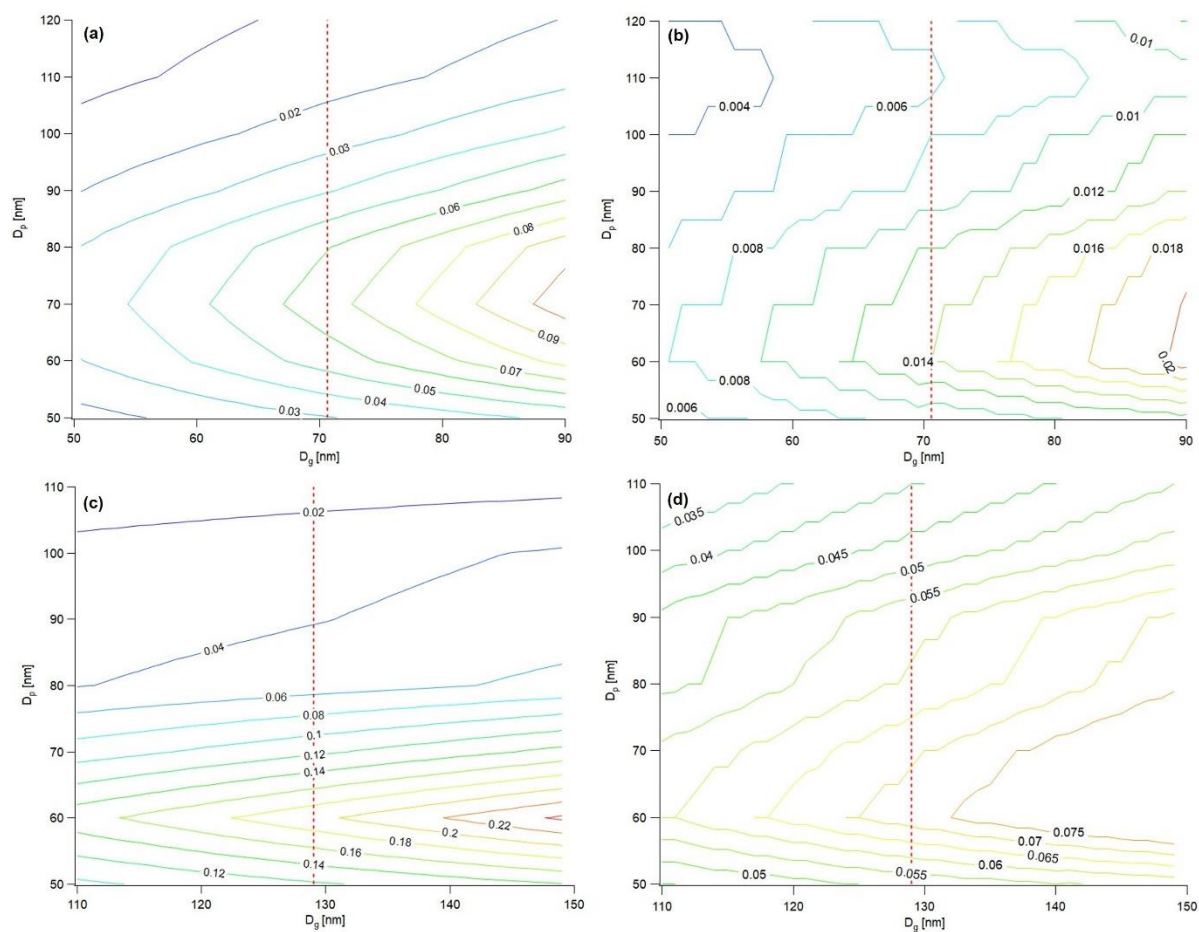


Figure 6: κ values as function of particle size before (filled square) and after (square) correction for Case I (black) and Case II (red).



355 **Figure 7: The deviation (Original value – Corrected value) of F_{act} ((a) for Case I and (c) for Case II) and κ ((b) for Case I and (d) for Case II) as function of D_g for log-normally fitted particle size distribution. Contour indicates the range of relative deviation and the value is marked on the contour (The redder the color of the contour, the greater the value). Red dashed line presents the original D_g value for each case ($D_g = 70.6$ nm for Case I and $D_g = 129.0$ nm for Case II).**